

COMPARATIVE STUDY OF LINEARIZED AND NON-LINEARIZED MODIFIED LANGMUIR ISOTHERM MODELS ON ADSORPTION OF ASPHALTENE ONTO MINERAL SURFACES

M. Mohammadi*, M.J. Ameri Shahrabi*, M. Sedighi**

*Department of Petroleum Engineering, Amirkabir University (Tehran polytechnic), Tehran, Iran

**Department of Chemical Engineering, Tarbiat Modares University, Tehran, Iran

majidmohammadi88@yahoo.com

In this paper, the Langmuir isotherm, originally derived for the adsorption of asphaltene extracted from shale oil and dissolved in toluene on Kaolin, Smectite, Fluorite and Hematite, was modified to fit the adsorption isotherm. The modified Langmuir isotherm parameters obtained from the four linear equations using the linear method differed. The aim of the proposed modification is based on the fact that direct application of the Langmuir isotherm often leads to poor data fitting. In the present communication, it is shown that the level of data fitting to the Langmuir isotherm can be improved by a simple modification through introducing a concentration dependent factor, X . The present paper discusses four modified Langmuir linearized isotherm models and one non-linear isotherm model: their coefficients are estimated and, for the study of non-linear isotherm model, genetic algorithm is used. A genetic algorithm procedure was utilized to optimize the modified Langmuir constants for a more accurate estimation of the set of model parameters. The obtained results demonstrated that the best fit was obtained using genetic algorithm. Furthermore, it was found out that from the surface minerals mentioned, Hematite mineral follows a multilayer adsorption isotherm.

УДК 541.183

INTRODUCTION

Asphaltenes are commonly described as a class of petroleum molecules that are insoluble in normal alkanes (n-pentane or n-heptane) but soluble in aromatics such as benzene or toluene [1, 2]. They are considered to be the most polar fraction of crude oil [3, 4]. Asphaltenes are a complex mixture of macromolecules with molecular weights (MW) that range from 500 up to 100,000 Da according to different authors and methods [5, 6]. Asphaltenes can undergo phase separation and deposition due to changes in temperature, pressure, and/or solution composition [2, 7] during production, transportation, and during the refining processes. Studies on asphaltene/mineral interactions yield new results in the field of environmental chemistry. During the enhanced oil recovery (EOR) procedures insoluble asphaltene particles may appear in the environment. They may also originate from uncontrolled split of oil products [8]. Therefore, understanding the mechanism of asphaltene deposition is a critical step in combating asphaltene deposition problem.

One of the most important changes is wettability alteration, where particles in contact with crude oil surface-active components (e.g. asphaltenes) will change from hydrophilic to hydrophobic (or less hydrophilic) [9–11]. The adsorption of asphaltenes onto minerals has been extensively studied [8, 12–16] because, as already mentioned, asphaltene adsorption on the formation rock alters the wettability of rocks [17] and reduces oil production from the reservoir. Also, in paper [18] asphaltenes (and a number of model compounds) were used for adsorption experiments (thermodynamic and kinetic) using Kaolin as an adsorbent. The results have indicated that the adsorption was governed by the presence of an aromatic framework, heteroatoms (nitrogen and oxygen), and to a lesser extent sulfur and a minor dependence on molecular weight [18].

Recently, Alboudwarej et al [19] have studied the adsorption of Athabasca and Cold Lake asphaltenes on stainless steel (304 L), iron, and aluminum powders using UV-vis spectrophotometry. The effects of resins, temperature, and n-heptane-to-toluene ratio were also investigated. In all cases, Langmuir isotherms were observed, indicating that asphaltenes saturated the surface area available for adsorption. The saturation adsorption of the asphaltenes on metals ($0.25\text{--}2.7\text{ mg m}^{-2}$) was of the same order of magnitude as that on minerals [14, 20].

Linear regression is frequently used to determine the best-fitting isotherm. The linear least-squares method with linearly transformed isotherm equations has also been widely applied to confirm experimental data and isotherms using a combination of relative error measure (e.g., R^2) and absolute error measure (e.g., RMSE).

Genetic algorithms (GAs) is a search technique used in computing to find exact or approximate solutions to optimization and search problems. Genetic algorithms are categorized as global search heuristics. In recent years, the concept of GAs has gained wide popularity in many areas of chemical and petroleum engi-

neering such as reservoir studies [21–23], optimization [24–26], polymerization process [27, 28], estimation of kinetic parameters [29–31] and biology [32, 33].

The goal of the present paper is to propose a modified Langmuir isotherm by which the level of data fitting in solution systems can be significantly improved. During modification we assumed that asphaltene concentration affects not only the adsorption stage but also the desorption step. To simplify the model we adopted a single-term polynomial in the description of the solute concentration dependence in both adsorption and desorption stages. The modified Langmuir isotherm has advantages compared with other isotherms. Better fit of the asphaltene adsorption was derived using a modified Langmuir isotherm. Furthermore, as will be detailed later, the magnitude of this single-term may be related to the level of surface heterogeneity and multilayer adsorption.

To our knowledge, there is no single article [2–4, 8, 10, 12–16, 19, 20, 34–36] on modification of Langmuir Isotherm for the adsorption of asphaltene onto mineral surfaces and most of the articles do not satisfy the multilayer adsorption of asphaltene and those articles use the original Langmuir adsorption. However, in the present paper we propose a new modified model for the Langmuir adsorption and indicate that some minerals follow Langmuir and others deviate a little from Langmuir and follow the modification of Langmuir. Based on this concept, we justify multilayer adsorption that the papers cited do not.

The present paper discusses four modified Langmuir linearized isotherm models and one non-linear isotherm model; their coefficients are estimated and, for the study of non-linear isotherm model, genetic algorithm is used.

1. MATERIALS AND METHODS

The sample of oil was extracted from bituminous shale oil from the Irati formation oil shale of the São Mateus do Sul deposit, in Paraná, Southern Brazil. The recovered oil was the fraction retained by the particles in the filter cake after the purification process. To separate this oil, the sludge was Soxhlet extracted with toluene, and the solvent then evaporated.

The asphaltenes were isolated from a sample of recovered shale oil using the ASTM 2007 standard procedure. Before use, the asphaltenes fraction was dissolved in toluene and filtered through a Millipore filter to eliminate the insoluble material. The preparation of four minerals (Kaolin, Smectite, Fluorite and Hematite) was shown in Gonzalez and Moreira [35].

The amount of asphaltenes adsorbed by f mineral was determined by measuring the reduction in concentration of the toluene solution of these fractions after four hours contact with the solid powder. The concentration was measured at the wavelength of 400 nm, using 10 mm optical path cells, with the double beam Varian 634 Spectrophotometer [35, 36].

2. MODIFICATION OF LANGMUIR ISOTHERM

2.1. LANGMUIR ISOTHERM

The chemical reaction for monolayer adsorption can be represented as follows:



where AS represents a solute molecule bound to a surface site on S . The equilibrium constant K for this reaction is given by:

$$K = \frac{[AS]}{[A][S]} \quad (2)$$

where $[A]$ denotes the concentration of A , while the other two terms $[S]$ and $[AS]$ are two dimensional analogs of concentration. The principle of chemical equilibrium holds with these terms. The complete form of the Langmuir isotherm considers (Eq. 2) in terms of the surface coverage θ which is defined as the fraction of the adsorption sites to which a solute molecule has become attached. An expression for the fraction of the surface with unattached sites is therefore $(1-\theta)$. Given these definitions, we can rewrite the term $[AS]/[S]$ as

$$\frac{[AS]}{[S]} = \frac{\theta}{1-\theta} \quad (3)$$

Now we express $[A]$ as C and finally:

$$\theta = \frac{KC}{1 + KC}. \quad (4)$$

If we define q as the amount of adsorption in units of moles adsorbate per mass adsorbant, and q_{max} and the maximal adsorption, then:

$$\theta = \frac{q}{q_{max}}. \quad (5)$$

Therefore,

$$q = \frac{q_{max}KC}{1 + KC}. \quad (6)$$

As mentioned before, the Langmuir isotherm is based on the three key assumptions: monolayer coverage, sites equivalence and sites independence. These premises may be oversimplified but in the case of gas adsorption on a well-defined solid surface, they are reasonable assumptions [37].

2.2. MODIFICATION OF LANGMUIR ISOTHERM

Sometimes, the adsorption of solutes on solid surface may not hold the above three premises. Two reasons underlie why with Langmuir's original isotherm for systems it is potentially problematic to describe the adsorption in solution systems. First, when a species is adsorbed from solution, there should be accompanying desorption of another species for charge-balance considerations [38]. Second, the existence of surface heterogeneity may cause an island-type adsorption, which clearly deviates from the important Langmuir pre-supposition of adsorption site equivalence [39].

In order to determine the modification of the Langmuir isotherm, the exact dependency of surface coverage on solute concentration of adsorption and desorption process, for example C^m and C^n , respectively, should be determined. This leads us to a modified Langmuir isotherm as follows:

$$\theta = \frac{KC^X}{1 + KC^X} \quad (7)$$

where C is the solute concentration, and $X(=m-n)$ is an exponent indicating the level of concentration dependence. Therefore, by equation 5, the above equation can be rearranged to:

$$q = \frac{q_{max}KC^X}{1 + KC^X}. \quad (8)$$

3. MODELING

3.1. REGRESSION

The Regression analysis tool performs linear regression analysis by using the least-squares method to fit a line through a set of observations. Regression can analyze how a single dependent variable is affected by the values of one or more independent variables. Linear regression is frequently used to determine the best-fitting isotherm, and the method of least squares has been used to find the parameters of the isotherms. In order to choose the best model for fitting experimental data, two kinds of isotherm have been utilized: the Langmuir and the modified Langmuir isotherms. However, the modified Langmuir isotherm can be linearized as four different types (see table 1), and simple linear regression will result in different parameter estimates [40, 41].

It is worth noting here that the exponent X is a fitting parameter by which we can determine the best linear regression for a given system.

Table 1. Linear and non-linear isotherm equations for modified Langmuir isotherms

Isotherm	Non-linear equation	Linear equation	Plot
Langmuir-1		$\frac{C^X}{q} = \frac{C^X}{q_{max}} + \frac{1}{Kq_{max}}$	$\frac{C^X}{q}$ vs. C^X
Langmuir-2		$\frac{1}{q} = \left(\frac{1}{Kq_{max}}\right) \frac{1}{C^X} + \left(\frac{1}{q_{max}}\right)$	$\frac{1}{q}$ vs. $\frac{1}{C^X}$
	$q = \frac{q_{max} KC^X}{1 + KC^X}$		
Langmuir-3		$q = q_{max} - \left(\frac{1}{K}\right) \left(\frac{q}{C^X}\right)$	q vs. $\frac{q}{C^X}$
Langmuir-4		$\frac{q}{C^X} = Kq_{max} - Kq$	$\frac{q}{C^X}$ vs. q

*This table is the same as Langmuir isotherm equations when $X = 1$.

3.2. GENETIC ALGORITHMS

The GAs could optimize linear and nonlinear objective functions by exploring the space of problem and exponentially exploiting promising areas through selection, crossover, and mutation operations applied to individuals the population [42].

Taking into account advantages and limitations of GAs, it could be specified when a GA should be applied for optimization problems. Moreover it handles noisy functions well and is resistant to becoming trapped in local optima. But it should be remembered that a GA has some limitations like identifying fitness function, defining representation, premature convergency, problem of choosing various parameters like the size of the population, mutation rate, crossover rate, the selection method and number of elites and sometimes it needs to be coupled with a local search technique [43, 44]. What is nice when comparing GAs to other optimization methods is that the fitness function can be nearly anything that can be evaluated by a computer or even something that cannot.

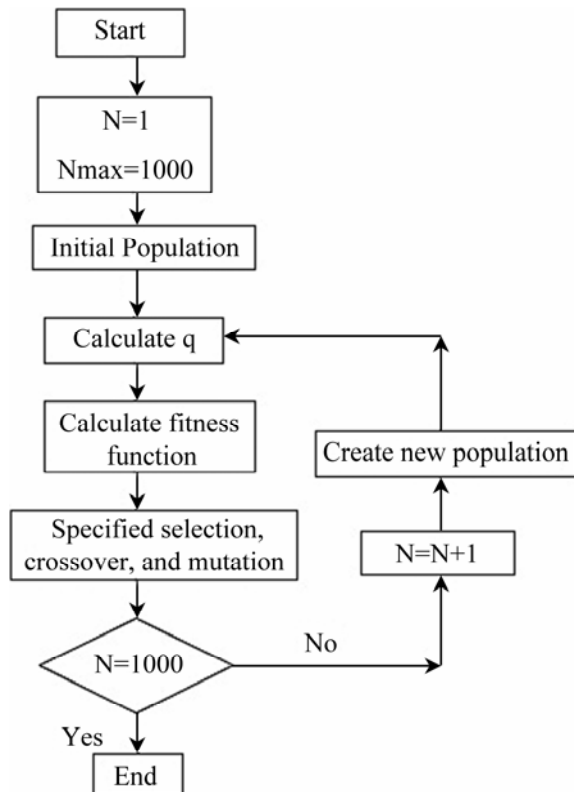


Fig. 1. Flowchart of used GA program

GAs operate with coded versions of the problem parameters rather than parameters themselves, i.e., a GA works with the coding of the solution set and not with the solution itself. Almost all conventional optimization techniques search from a single point but GAs always operate on a whole population of points (strings), i.e., a GA uses population of solutions rather than a single solution from those searched. This plays a major role to the robustness of GAs. It improves the chance of reaching the global optimum and also helps in avoiding local stationary point. GAs use fitness function for evaluation rather than derivatives. As a result, they can be applied to any kind of continuous or discrete optimization problems. The key point to be performed here is to identify and specify a meaningful decoding function. The general flowchart steps of the used computer program are presented in fig. 1.

Table 2 indicates the numerical parameter values used in GAs for all optimization runs. In this optimization, the rank method is used for fitness scaling, while stochastic uniform is used for the selection method to specify how the genetic algorithm chooses parents for the next generation.

Table 2. Computational Parameters of GA

Computational parameters	Values
Population size	100
Elite count	2
Crossover fraction	0.80
Number of generation	1000
Fitness scaling function	@fitscalingrank
Selection function	@selectionstochunif
Crossover function	@crossoverscattered
Mutation function	@mutationuniform
Mutation probability	0.05

4. RESULTS AND DISCUSSIONS

All calculation and GAs programming were carried out using MATLAB 7.7 mathematical software and Microsoft excel. As was proposed by Legates and McCabe [45], a perfect way of evaluating a model should contain a combination of relative error measures (e.g., R^2) and absolute error measure s(e.g., $RMSE$). In the present paper, R^2 and $RMSE$ were used to evaluate the performance of the model. R^2 and $RMSE$ are defined as below:

$$RMSE = \sqrt{MSE} \quad (9)$$

$$MSE = \frac{SSE}{n} \quad (10)$$

$$SSE = \sum_{i=1}^n (q_{exp,i} - q_{model,i})^2 \quad (11)$$

$$R^2 = 1 - \frac{SSE}{SST} \quad (12)$$

$$SST = \sum_{i=1}^n (q_{exp,i} - \bar{q}_{exp})^2 \quad (13)$$

where MSE , SSE and SST are the mean squared error, the sum of squared error and the sum squared total, respectively. And n , $q_{model,i}$ and $q_{exp,i}$ are the number of experimental points, the predicted amount of asphaltene adsorbed on the mineral surface by the model and results of experiments, respectively.

Modified Langmuir coefficients for four linearized modified Langmuir equations were obtained by plotting graphs between C^x/q versus C^x (Type-I linearized equation), $1/q$ versus $1/C^x$ (Type-II linearized equation), q versus q/C^x (Type-III linearized equation), and q/C^x versus q (Type-IV linearized equation) The calculated parameters for three arbitrary X are shown in table 3. When $X = 1$, the modified isotherm returns to the original form of the Langmuir isotherm.

From table 3, it can be inferred that different linear modified Langmuir equations show different Langmuir constants, as indicated by variation in errors. In all cases of Kaolin, Smectite, Fluorite and Hematite, through the comparison of the four linearized modified Langmuir equations, it is observed that the Type-I linearized modified Langmuir equation showed a higher value of the correlation coefficient than that of the other three linearized equations (Type-II to IV), as shown in table 3.

The adsorption capacities of various minerals differ with each other by changing the type of linearization. For example, the adsorption capacity of Kaolin was found to be 1.9139 mg/m² for Type-I linearized modified Langmuir ($X = 1$) and that of Type-II, III and IV are 1.943 mg/m², 1.6297 mg/m² and 2.045 mg/m², respectively. In other words, the transformation of a non-linear isotherm model to a linear isotherm model seems to implicitly alter the error functions, as well as the error variance and normality assumptions of the least-squares method [40, 46].

Table 3. Linear regression equations of Modified Langmuir Isotherm

<i>X</i>	<i>Modified Langmuir Isotherm</i>	<i>Equation (y =)</i>	<i>R</i> ²	<i>RMSE</i>	<i>q</i> _{max} (mg/m ²)	<i>K</i> (dm ³ /mg)
<i>Kaolin</i>						
0.8	Type 1	0.4321x+39.024	0.987	1.18	2.3143	0.0111
	Type 2	28.529x+0.5909	0.975	1.66	1.6921	0.0207
	Type 3	-44.821x+1.687	0.977	1.57	1.6871	0.0223
	Type 4	-0.01x + 0.0265	0.981	1.44	2.650	0.0101
1	Type 1	0.5225x + 77.194	0.990	1.025	1.9139	0.0068
	Type 2	51.864x + 0.51479	0.984	1.34	1.943	0.00992
	Type 3	-95.401x + 1.6297	0.987	1.18	1.6297	0.0105
	Type 4	-0.0067x + 0.0137	0.988	1.15	2.045	0.0067
1.2	Type 1	0.5605x + 188.72	0.986	1.24	1.7841	0.00297
	Type 2	170.713x + 0.5121	0.981	1.45	1.9525	0.00299
	Type 3	-248.663x + 1.5639	0.983	1.36	1.564	0.00402
	Type 4	-0.00485x + 0.0087	0.987	1.19	1.794	0.00485
<i>Smectite</i>						
0.8	Type 1	2.474x + 84.903	0.942	1.0556	0.4042	0.0291
	Type 2	114.509x + 2.265	0.909	1.0697	0.4415	0.0198
	Type 3	-44.643x + 0.427	0.92	1.0654	0.427	0.0224
	Type 4	-0.0194x +0.08604	0.907	1.0704	0.444	0.0194
1	Type 1	2.6246x + 154.392	0.962	1.0449	0.381	0.017
	Type 2	260.145x + 2.141	0.921	1.0648	0.467	0.00823
	Type 3	-23.362x + 0.4118	0.938	1.0575	0.412	0.043
	Type 4	-0.0404x + 0.01706	0.934	1.0591	0.422	0.0404
1.4	Type 1	2.532x + 192.255	0.948	1.0526	0.395	0.01317
	Type 2	283.364x + 2.153	0.902	1.0723	0.4645	0.0076
	Type 3	-105.263x + 0.4416	0.916	1.0668	0.4416	0.0095
	Type 4	-0.0099x + 0.00437	0.912	1.0684	0.4413	0.0099
<i>Fluorite</i>						
0.8	Type 1	0.34835x + 26.813	0.951	1.273	2.8706	0.0179
	Type 2	22.4815x + 0.4882	0.919	1.352	2.047	0.0217
	Type 3	-61.1955x + 2.4603	0.939	1.305	2.4603	0.0163
	Type 4	-0.0153x + 0.04016	0.95	1.276	2.625	0.0153
1	Type 1	0.39039x + 66.894	0.946	1.286	2.5614	0.00583
	Type 2	23.922x + 0.72601	0.903	1.385	1.3773	0.03034
	Type 3	-32.215x + 1.5432	0.935	1.315	1.5432	0.03104
	Type 4	-0.0228x + 0.05041	0.939	1.305	2.211	0.0228
1.6	Type 1	0.4596x + 209.357	0.912	1.366	2.176	0.00219
	Type 2	43.9543x + 1.0324	0.816	1.530	0.968	0.0235
	Type 3	-113.26x + 1.049	0.846	1.486	1.049	0.00882
	Type 4	-0.0029x + 0.00453	0.862	1.459	1.5631	0.0029
<i>Hematite</i>						
0.8	Type 1	0.2077x + 22.625	0.791	4.988	4.817	0.00918
	Type 2	28.689x + 0.2083	0.741	5.062	4.8012	0.00726
	Type 3	-113.507x + 4.2811	0.721	5.0005	4.2811	0.00881
	Type 4	-0.00667x + 0.0319	0.728	5.026	4.7961	0.00667
1	Type 1	0.17819x + 72.79	0.85	4.665	5.6119	0.00245
	Type 2	86.637x + 0.18679	0.802	4.732	5.3536	0.00215
	Type 3	-581.057x + 5.8089	0.787	4.771	5.8089	0.00172
	Type 4	-0.00201x + 0.0109	0.792	4.747	5.445	0.00201
1.6	Type 1	0.1821x + 791.74	0.97	1.656	5.491	0.00023
	Type 2	667.345x + 0.1835	0.967	1.689	5.4489	0.00027
	Type 3	-1886.79x + 5.3198	0.929	2.02	5.3198	0.00053
	Type 4	-0.00036x + 0.0019	0.955	1.8103	5.389	0.00036

Figure 2 indicates the R^2 versus X for different mineral surfaces for the best fit (Type I). For Kaolin, Smectite, Fluorite and Hematite, it is apparent that the best linear fit, represented by the highest R^2 , is obtained when X is equal to 1, 1, 0.8 and 1.6, respectively. Above or below the optimized X for each mineral surface, R^2 decreases from its maximum value. $X = 1$ shows that the adsorption isotherm follows the Langmuir isotherm. Therefore, Kaolin and Smectite follow the Langmuir isotherm, indicating that there is the monolayer formation of adsorbed asphaltenes onto the surface. In addition, for Fluorite, R^2 is equal to 0.946 when $X = 1$ but $R^2 = 0.951$ when $X = 0.8$. It indicates that there is a little deviation from the Langmuir isotherm. For Hematite, the maximum value of R^2 occurs at $X = 1.6$, which is significantly higher than $X = 1.0$, indicating the multilayers formation of asphaltenes onto the surface. The Multilayer formation is closely related to the aggregate formation and precipitation of asphaltenes in the bulk [47]. For this mineral, the adsorption behavior is different, showing a lower adsorption for low concentrations of asphaltenes and a marked increase for intermediate concentrations.

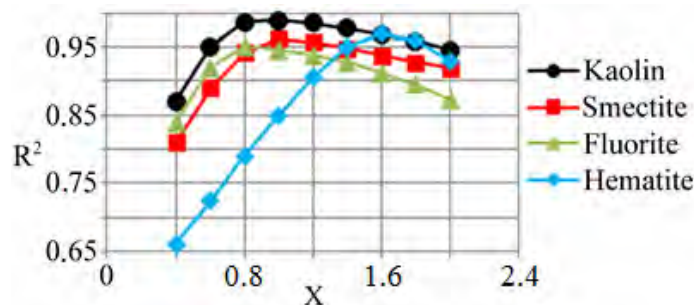


Fig. 2. R^2 versus X for linear regression for different mineral surfaces

Figures 3 and 4 give the plots of the comparison of the observed data for Fluorite, Smectite, Kaolin and Hematite at their optimum X with the experimental data. It is shown that there is good agreement between model and experimental values. For Smectite and Kaolin, $X = 1$ indicates that they follow the Langmuir isotherm. However, a high deviation from the Langmuir model for Hematite shows that it does not follow the monolayer adsorption.

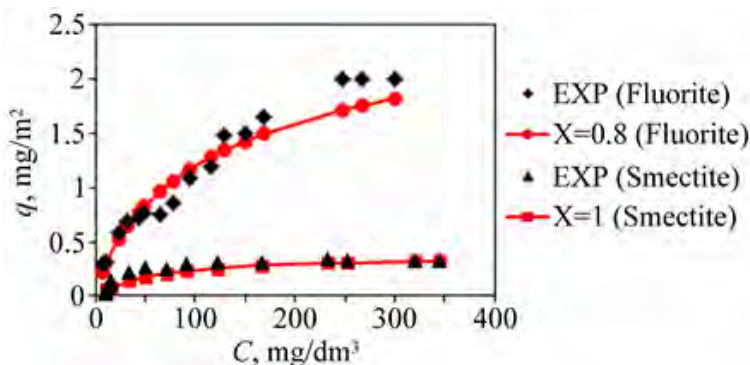


Fig. 3. Modified Langmuir linearized isotherm model for Fluorite and Smectite at their optimum X

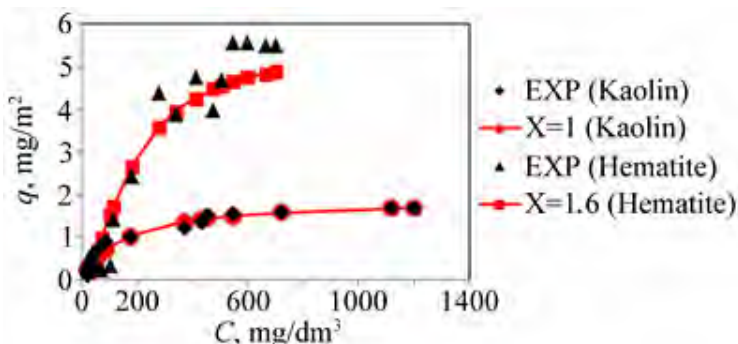


Fig. 4. Modified Langmuir linearized isotherm model for Kaolin and Hematite at their optimum X

For Fluorite, there is a little difference between R^2 and RMSE of the two set of $X = 0.8$ and $X = 1$. It means there is a slight surface heterogeneity and a tendency to ideal surface (0 for extremely heterogeneous, and 1 for an ideal homogeneous surface).

Figures 5 and 6 present the scatter diagrams for mineral surfaces for linear regression. As mentioned above, there is a deviation between the model and the experimental values for Hematite at $X = 1$. Figures indicate overall favorable agreement between the predicted and the experimental data at optimum X for different mineral surfaces.

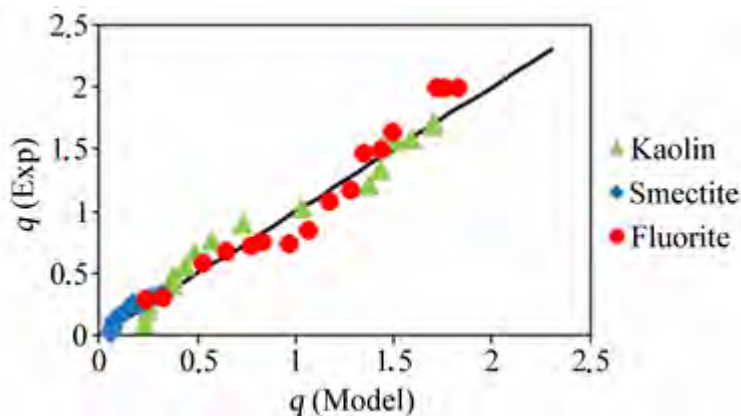


Fig. 5. Scatter diagram for linear regression for Kaolin, Smectite and Fluorite

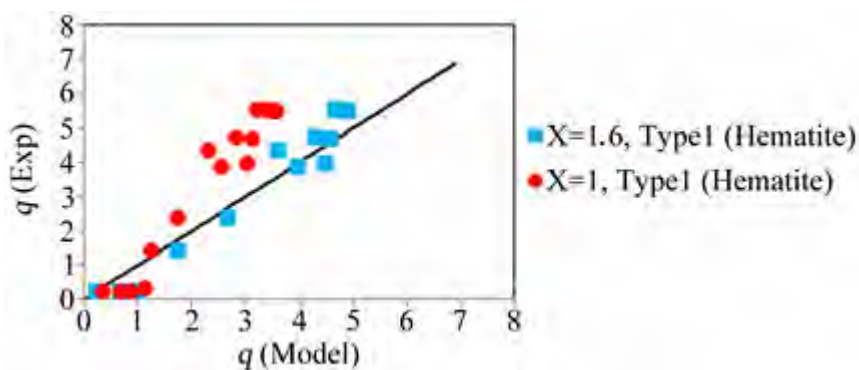


Fig. 6. Scatter diagram for linear regression for Hematite

In the present paper, to study the non-linear isotherm model, a GA was used to determine the non-linear coefficients. The optimized parameters (q_{max} , b and X) are shown in table 4. Accordingly, a plot of R^2 versus X (fig. 7) and plots of the comparison of the observed data by non-linear models for Fluorite, Smectite, Kaolin and Hematite at their optimum X with the experimental data (figs. 8, 9) were drawn.

Table 4. Non-linearized isotherm parameters

Mineral	$q_{max}(mg/m^2)$	$K(dm^3/mg)$	X	RMSE	R^2	Runtime Langmuir (sec)
Kaolin	1.8008	0.00925	0.991	0.779	0.993	7.51
Smectite	0.337	0.012005	1.395	0.894	0.99	7.32
Fluorite	2.7398	0.009199	0.982	0.811	0.992	7.33
Hematite	6.5981	0.00015	1.581	1.362	0.985	9.04

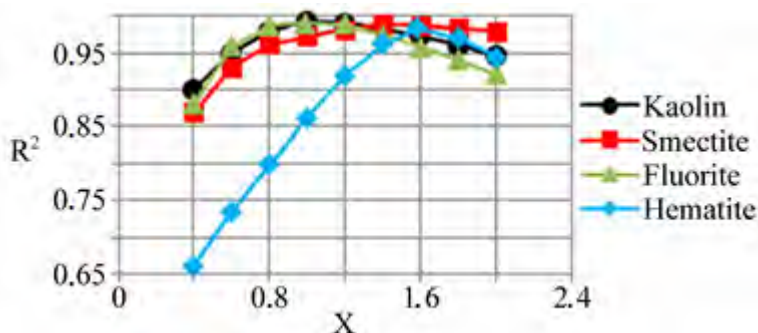


Fig. 7. R^2 versus X for non-linear for different mineral surfaces

The optimized coefficients for different surface minerals are shown in table 4. Figure 7 demonstrates that for X for Kaolin, Smectite, Fluorite and Hematite the best values are 0.991, 1.395, 0.982 and 1.581, respectively. In these optimized X , R^2 is 0.993, 0.99, 0.992 and 0.985 and $RMSE$ is 0.779, 0.894, 0.811 and 1.362, respectively.

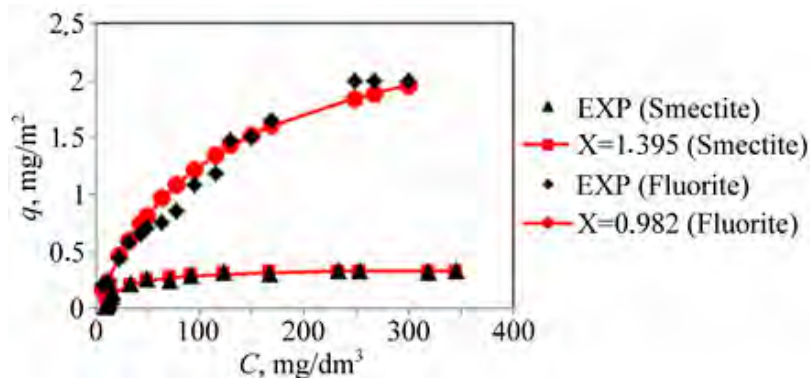


Fig. 8. Modified Langmuir non-linearized isotherm models for Smectite and Fluorite at their optimum X

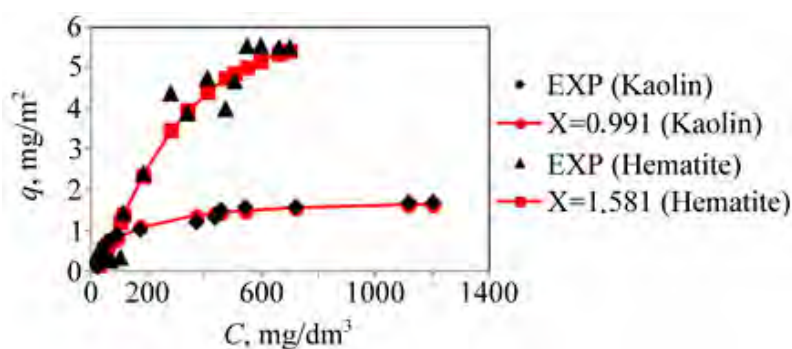


Fig. 9. Modified Langmuir non-linearized isotherm models for Kaolin and Hematite at their optimum X

From figs. 8 and 9, we conclude that the non-linear isotherm models can fit experimental data better than linear regression. Kaolin and Fluorite follow the Langmuir isotherm.

For Smectite, in linear regression, the optimum X was equal to 1, which means that it followed the monolayer adsorption. However, in the non-linear regression, the amount of X is optimized to 1.395, which indicates that there is some tendency to the multilayer adsorption. In addition, for $X = 1$, the amount of R^2 is equal to 0.973 which is 1.7% lower than the optimized value (for $X = 1.395$, $R^2 = 0.99$).

Figure 9 indicates that Hematite follow the multilayer adsorption, because the best result is attained at $X = 1.581$, while at $X = 1$, the amounts of R^2 and $RMSE$ are equal to 0.863 and 4.029, respectively.

Figures 10 and 11 present the scatter diagrams for mineral surfaces for the non-linear regression. They show good agreement between the predicted and experimental data.

The comparison between the four types of linearized isotherm models and a non-linear isotherm for different mineral surfaces at their optimum X is shown in table 5. It is clear that among all the types of linear isotherms, type 1 is better than the others (highest R^2 and lowest $RMSE$). However, a non-linear isotherm can fit experimental data better than a linear isotherm. The non-linear method is a better way to obtain the isotherm parameters.

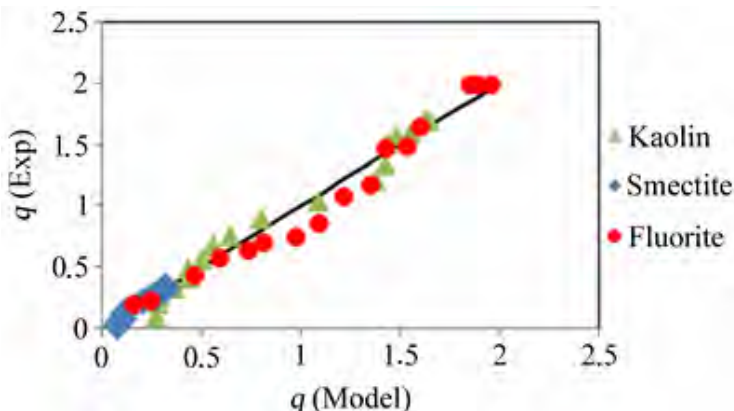


Fig. 10. Scatter diagram for non-linear isotherm for Kaolin, Smectite and Fluorite

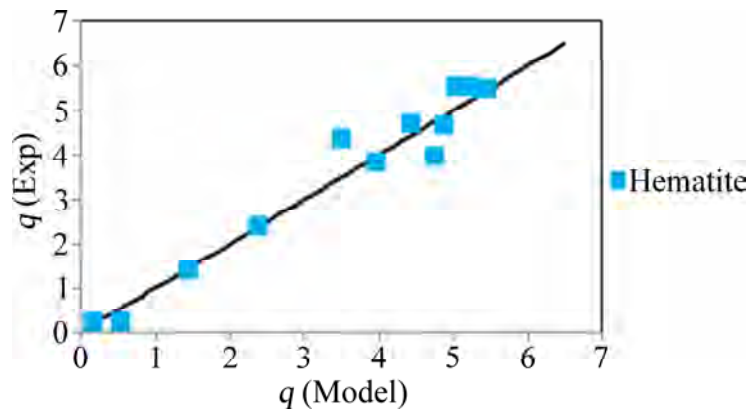


Fig. 11. Scatter diagram for non-linear isotherm for Hematite

Table 5. Comparison of linearized and non-linearized isotherms

X	Modified Langmuir Isotherm	R^2	RMSE
<i>Kaolin</i>			
1	Linear-Type1	0.9905	1.025
	Linear-Type 2	0.984	1.34
	Linear-Type 3	0.987	1.18
	Linear-Type 4	0.988	1.15
0.991	Non-Linear	0.993	0.779
<i>Smectite</i>			
1	Linear-Type1	0.962	1.0449
	Linear-Type 2	0.921	1.0648
	Linear-Type 3	0.938	1.0575
	Linear-Type 4	0.934	1.0591
1.395	Non-Linear	0.99	0.894
<i>Fluorite</i>			
0.8	Linear-Type1	0.951	1.273
	Linear-Type 2	0.919	1.352
	Linear-Type 3	0.939	1.305
	Linear-Type 4	0.95	1.276
0.982	Non-Linear	0.992	0.811
<i>Hematite</i>			
1.6	Linear-Type1	0.97	1.656
	Linear-Type 2	0.967	1.689
	Linear-Type 3	0.929	2.02
	Linear-Type 4	0.955	1.8103
1.581	Non-Linear	0.985	1.362

When X is smaller than 1, the particular adsorbate/adsorbent system exhibits less concentration dependence; while, when X is greater than 1, the system experiences higher concentration dependence. In other words, to obtain the same level of surface coverage (or adsorption amount), the system of $X < 1$ requires less amount of solute, while the $X > 1$ system mandates more. Sometimes, X can be negative for some cases, which means that for $X < 0$, the term $(m-n)$ must be negative (i.e., $m < n$), which means the solute concentration effect upon desorption stage is stronger than that in adsorption stage [39].

5. CONCLUSION

The Langmuir isotherm was modified to fit the adsorption isotherm of asphaltene onto mineral surfaces. Langmuir-type 1 is the most-popular linear form which had the highest coefficient of determination

compared with other Langmuir linear equations. However, it is always better to find the isotherm coefficients by non-linear method, and more practicable. The results of linear and non-linear isotherms indicate that Kaolin, Smectite and Fluorite follow the Langmuir isotherm, while Hematite mineral follows the multilayer adsorption isotherm. However, for Smectite, there is some tendency to the multilayer adsorption.

NOMENCLATURE

GA – genetic algorithm; θ – the amount of adsorption per the maximum adsorption; *MSE* – mean squared error; *SSE* – sum squared error; *SST* – sum squared total; *n* – number of experimental points; $q_{exp,i}$ [mg/m²] – amount of asphaltene adsorbed on the mineral surface by the results of experiments; $q_{model,i}$ [mg/m²] – amount of asphaltene adsorbed on the mineral surface by the model; N_{max} – Number of generation; q_{max} [mg/m²] – maximum amount of adsorbed asphaltene; K [dm³/mg] – Langmuir constant, ratio of the adsorption rate constant to the desorption rate constant; q [mg/m²] – amount of asphaltene adsorbed on the mineral surface; C [mg/dm³] – the equilibrium concentration of asphaltene solution.

REFERENCES

1. Speight J.G. The Chemistry and Technology of Petroleum. CRC Press: Boca Raton, FL, 1999.
2. Rudrake A., Karan K., Horton J.H. A Combined QCM and XPS Investigation of Asphaltene Adsorption on Metal Surfaces. *Journal of Colloid and Interface Science*. 2009, **332**, 22–31.
3. (a) Syunyaev R.Z., Balabin R.M., Akhatov I.S., Safieva J.O. Adsorption of Petroleum Asphaltenes onto Reservoir Rock Sands Studied by Near-Infrared (NIR) Spectroscopy. *Energy Fuels*. 2009, **23**, 1230–1236. (b) Balabin R.M., Safieva R.Z., Lomakina E.I. Comment on Enthalpy Difference between Conformations of Normal Alkanes: Raman Spectroscopy Study of n-Pentane and n-Butane. *Anal. Chim. Acta*. 2010, **671**, 27–35.
4. (a) Mullins O.C., Sheu E.Y., Hammami A., Marshall A.G. *Asphaltenes, Heavy Oils, and Petroleomics*. 1st ed.; Springer: New York, 2006. (b) Labrador H., Fernández Y., Tovar J., Muñoz R., Pereira J.C. Ellipsometry Study of the Adsorption of Asphaltenes Films on Glass Surface. *Energy & Fuels*. 2007, **21**, 1226–1230. (c) Jouault N., Corvis Y., Cousin F., Jestin J., Barr L. Asphaltene Adsorption Mechanisms on the Local Scale Probed by Neutron Reflectivity: Transition from Monolayer to Multilayer Growth above the Flocculation Threshold. *Langmuir*. 2009, **25**, 3991–3998.
5. Groenzin H., Mullins O.C. Asphaltene Molecular Size and Structure. *J. Phys. Chem. A*. 1999, **103**, 11237–11245.
6. Groenzin H., Mullins O.C. Molecular Size and Structure of Asphaltenes from Various Sources. *Energy Fuels*. 2000, **14**, 677–684.
7. Hammami A., Phelps C.H., Monger-McClure T., Little T.M. Asphaltene Precipitation from Live Oils: An Experimental Investigation of Onset Conditions and Reversibility. *Energy Fuels*. 2000, **14**, 14–18.
8. Marczewski A.W., Szymula M. Adsorption of Asphaltenes from Toluene on Mineral Surface. *Colloids Surfaces A–Physicochem. Eng. Aspects*. 2002, **208**, 259–266.
9. Gu G., Zhou Z., Xu Z., Masliyah J.H. Role of fine Kaolin Clay in Toluene-diluted Bitumen/Water Emulsion. *Colloids Surfaces A–Physicochem. Eng. Aspects*. 2003, **215**, 141–153.
10. Hannisdal A., Ese M.H., Hemmingsen P.V., Sjöblom J. Particle-stabilized Emulsions: Effect of Heavy Crude Oil Components Pre-adsorbed onto Stabilizing Solids. *Colloids Surfaces A–Physicochem. Eng. Aspects*. 2006, **276**, 45–58.
11. Yan N.X., Masliyah J.H. Characterization and Demulsification of Solids-stabilized Oil-in-water Emulsions Part 2. Demulsification by the Addition of Fresh Oil. *Colloids Surfaces A–Physicochem. Eng. Aspects*. 1995, **96**, 243–252.
12. Acevedo S., Ranaudo M.A., Escobar G., Gutierrez L., Ortega P. Adsorption of Asphaltenes and Resins on Organic and Inorganic Substrates and their Correlation with Precipitation Problems in Production Well Tubing. *Fuel*. 1995, **74**, 595–598.
13. Acevedo S., Ranaudo M.A., Garcia C., Castillo J., Fernandez A., Caetano M., Goncalvez S. Importance of Asphaltene Aggregation in Solution in Determining the Adsorption of this Sample on Mineral Surfaces. *Colloids Surfaces A–Physicochem. Eng. Aspects*. 2000, **166**, 145–152.
14. Acevedo S., Ranaudo M.A., Garcia C., Castillo J., Fernández A. Adsorption of Asphaltenes at the Toluene-silica Interface: a Kinetic Study. *Energy & Fuels*. 2003, **17**, 257–261.
15. Kokal S., Tang T., Schramm L., Sayegh S. Electrokinetic and Adsorption Properties of Asphaltenes. *Colloids Surfaces A–Physicochem. Eng. Aspects*. 1995, **94**, 253–265.
16. Pernyeszi T., Patzko A., Berkesi O., Dekany I. Asphaltene Adsorption on Clays and Crude Oil Reservoir Rocks. *Colloids Surfaces A–Physicochem. Eng. Aspects*. 1998, **137**, 373–384.

17. Buckley J.S. Wetting Alteration of Solid Surfaces by Crude Oils and their Asphaltenes. *Revue De L Institut Francais Du Petrole*. 1998, **53**, 303–312.
18. López-Linares F., Carboognani L., González M.F., Sosa-Stull C., Figueras M., Pereira-Almao P. Quinolin-65 and Violanthrone-79 as Model Molecules for the Kinetics of the Adsorption of C7 Athabasca Asphaltenes on Macroporous Solid Surfaces. *Energy&Fuel*. 2006, **20**, 2748–2750.
19. Alboudwarej H., Pole D., Svrcek W.Y., Yarranton H.W. Adsorption of Asphaltenes on Metals. *Ind. Eng. Chem. Res.* **2005**, *44*, 5585–5592.
20. Mendoza dela Cruz J.L., Castellanos-Ramirez I.V., Ortiz-Tapia A., Buenrostro-Gonzalez E., Duran-Valencia C.A., Lopez-Ramirez S. Study of Monolayer to Multilayer Adsorption of Asphaltenes on Reservoir Rock Minerals. *Colloids Surfaces A*. 2009, **340**, 149–154.
21. Romero C.E., Carter J.N. Using Genetic Algorithms for Reservoir Characterization. *Journal of Petroleum Science and Engineering*. 2001, **31**, 113–123.
22. Romero, C.E., Carter, J.N. Using Genetic Algorithms for Reservoir Characterization. *Developments in Petroleum Science*. 2003, **51**, 323–363.
23. Saemi M., Ahmadi M., Yazdian Varjani A. Design of Neural Networks Using Genetic Algorithm for the Permeability Estimation of the Reservoir. *Journal of Petroleum Science and Engineering*. 2007, **59**, 97–105.
24. Nassif N., Kajl S., Sabourin R. Optimization of HVAC, Control System Strategy Using Two-objective Genetic Algorithm. *HVAC&R*. 2005, **11**(3), 459–486.
25. Wen-Sheng C., Fang Y., Xue-Guang S., Zhong-Xiao P. Geometry Optimizations of Benzene Clusters Using a Modified Genetic Algorithm. *Chinese Journal of Chemistry*. 2000, **18**(4), 475–481.
26. Mehrpooya M., Vatani A., Mousavian S.M.A. Optimum Design of Integrated Liquid Recovery Plants by Variable Population Size Genetic Algorithm. *Can. J. Chem. Eng.* 2010, **88**, 1054–1064.
27. Mat Noor R.A., Ahmad Z., Mat Don M., Uzir M.H. Modelling and Control of Different Types of Polymerization Processes Using Neural Networks Technique: A review. *Can. J. Chem. Eng.* 2010, **88**, 1065–1084.
28. Silva C.M., Biscaia Jr E.C. Genetic Algorithm Development for Multi-objective Optimization of Batch Free-radical Polymerization Reactors. *Computers & Chemical Engineering*. 2003, **27**, 1329–1344.
29. Saha B.P., Reddy K., Ghoshal A.K. Hybrid Genetic Algorithm to Find the Best Model and the Globally Optimized Overall Kinetics Parameters for Thermal Decomposition of Plastics. *Chemical Engineering Journal*. 2008, **138**, 20–29.
30. Feng G., Li F., Li H., Qu H., Cui Y. A Hybrid Genetic Algorithm for the Estimation of Polyesterification Kinetic Parameters. *Chemical Engineering & Technology*. 2006, **29**, 740–743.
31. Kadiva A., Taghi Sadeghi M., Sotudeh-Gharebagh R., Mahmudi M. Estimation of Kinetic Parameters for Hydrogenation Reactions Using a Genetic Algorithm. *Chemical Engineering & Technology*. 2009, **32**, 1588–1594.
32. Dhurjati P., Mahadevan R. Systems Biology: The Synergistic Interplay between Biology and Mathematics. *Can. J. Chem. Eng.* 2008, **86**, 127–141.
33. Webe L. Applications of Genetic Algorithms in Molecular Diversity. *Current Opinion in Chemical Biology*. 1998, **2**, 381–385.
34. Dudasova D., Simon S., Hemmingsen P.V., Sjoblom J. Study of Asphaltenes Adsorption onto Different Minerals and Clays: Part 1. Experimental Adsorption with UV Depletion Detection. *Colloids and Surfaces A: Physicochem. Eng. Aspects*. 2008, **317**, 1–9.
35. Gonzalez G., Moreira M.B.C. The Wettability of Mineral Surfaces Containing Adsorbed Asphaltenes. *Colloids and Surfaces*, 1991, **58**, 293–302.
36. Gonzalez G., Middea A. The Properties of the Calcite-Solution Interface the Presence of Adsorbed Resins or Asphaltenes. *Colloids and Surfaces*. 1988, **33**, 217–229.
37. Bawn C.E.H. The Adsorption of Gases and Vapors on Plane Surfaces. *J. Am. Chem. Soc.* 1932, **54**, 72–86.
38. Harter R.D., Baker D.E. Applications and Misapplications of the Langmuir Equation to Soil Adsorption Phenomena. *Soil Sci. Soc. Am. J.* 1977, **41**, 1077.
39. Sohn S., Kim D. Modification of Langmuir Isotherm in Solution Systems-definition and Utilization of Concentration Dependent Factor. *Chemosphere*. 2005, **58**, 115–123.
40. Kinniburgh D.G. General Purpose Adsorption Isotherms. *Environ. Sci. Technol.* 1986, **20**, 895–904.
41. Longhinotti E., Pozza F., Furlan L., Sanchez M.D.N.D., Klug M., Laranjeira M.C.M., Favere V.T. Adsorption of Anionic Dyes on the Biopolymer Chitin. *J. Braz. Chem. Soc.* 1998, **9**, 435–440.
42. Michalewicz Z. *Genetic Algorithms + Data Structures = Evolution Programs*. Springer-Verlag, New York, 1996.
43. Koza J.R. *Genetic Programming*. MIT Press, Cambridge, MA, 1992.

44. Sivanandam S.N., Deepa S.N. *Introduction to Genetic Algorithms*. Springer-Verlag, Berlin Heidelberg, 2008.
45. Legates D.R., McCabe Jr.G. Evaluating the Use of Goodness of Fit Measures in Hydrologic and Hydroclimatic Model Validation. *J. Water Resour. Res.* 1999, **35**, 233–241.
46. Ho Y.S., Wang C.C. Pseudo-isotherms for the Sorption of Cadmium Ion onto Tree Fern. *Proc. Biochem.* 2004, **39**, 761–765.
47. Castillo J., Fernandez A., Ranaudo M.A., Acevedo S. New Techniques and Methods for the Study of Aggregation, Adsorption, and Solubility of Asphaltenes. Impact of these Properties on Colloidal Structure and Flocculation. *Petrol. Sci. Technol.* 2001, **19**, 75–106.

Received 30.09.11

Реферат

В статье рассматривается модифицированная изотерма Ленгмюра, первоначально разработанная для адсорбции асфальтенов, извлеченных из сланцевого масла и растворенных в толуоле, на каолине, смектитах, флюорите и гематите. Параметры модифицированной изотермы Ленгмюра, полученные с помощью четырех линейных уравнений с использованием линейного метода оказались различными. Предлагаемая модификация обоснована тем фактом, что прямое использование изотермы Ленгмюра приводит к недостаточному соответствию данных. В данной статье показано, что можно добиться улучшения соответствия данных простой модификацией, с введением коэффициента концентрации X . Представлены четыре модели модифицированной линеаризованной изотермы Ленгмюра и одна модель нелинеаризованной изотермы Ленгмюра для сравнения коэффициентов концентрации; для исследования нелинеаризованной формы применяется генетический алгоритм. Этот алгоритм применяется для оптимизации модифицированных констант Ленгмюра с целью более точной оценки параметров модели. Полученные результаты демонстрируют, что наилучшее соответствие адсорбционных данных дает именно применение генетического алгоритма. Кроме того, было выявлено, что только поверхность гематита, из всех упомянутых выше минералов, дает на графике изотерму многослойной адсорбции.
